Biochemical and Biophysical Research Communications xxx (xxxx) 150393

Contents lists available at ScienceDirect

Biochemical and Biophysical Research Communications

journal homepage: www.elsevier.com/locate/ybbrc

Inhibition of early RNA replication in Chikungunya and Dengue virus by lycorine: In vitro and in silico studies

Tanvi Agrawal [a, b, *], Gazala Siddqui [b, 1], Ridhima Dahiya [c, 1], Aanchal Patidar [a], Upasna Madan [a], Supratik Das [b], Shailendra Asthana [c], Sweety Samal [b], Amit Awasthi [a, **]

[a] Centre for Immunobiology and Immunotherapy, Translational Health Science and Technology Institute, NCR-Biotech Science Cluster, 3rd Milestone, Faridabad, 121001, Haryana, India

[b] Centre for Virus Research, Therapeutics and Vaccines, Translational Health Science and Technology Institute, NCR-Biotech Science Cluster, 3rd Milestone, Faridabad, 121001, Haryana, India

[c] Computational Biophysics and CADD Group, Computational and Mathematical Biology Centre (CMBC), Translational Health Science and Technology Institute, NCR-Biotech Science Cluster, 3rd Milestone, Faridabad, 121001, Haryana, India

ARTICLE INFO

Keywords:
Chikungunya
Dengue
Lycorine
RNA dependent RNA polymerase
Antiviral
Natural product

ABSTRACT

Arboviruses such as chikungunya virus (CHIKV) and dengue virus (DENV) collectively afflict millions of individuals worldwide particularly in endemic countries like India, leading to substantial morbidity and mortality. With the lack of effective vaccines for both CHIKV and DENV in India, the search for antiviral compounds becomes paramount to control these viral infections. In line with this, our investigation was focused on screening natural compounds for their potential antiviral activity against CHIKV and DENV. Using different assays, including plaque assay, immunofluorescence, and reverse transcription-quantitative real-time PCR (qRT-PCR), out of 109 natural compounds tested, we confirmed lycorine's in vitro antiviral activity against CHIKV and DENV at low micromolar concentrations in different cell types. Time of addition assays indicated that lycorine does not impede viral entry. Additionally, qRT-PCR results along with time of addition assay suggested that lycorine interferes with the synthesis of negative strand viral RNA. Molecular docking analysis was done to understand the mode of inhibition of viral replication. The results revealed that the most likely binding site with the highest binding affinity of lycorine, was at the palm and finger domains, in the vicinity of the catalytic site of CHIKV and DENV RNA-dependent RNA polymerase (RdRp). Collectively, our data underscores the potential of lycorine to be developed as a direct acting inhibitor for DENV and CHIKV, addressing the critical need of requirement of an antiviral in regions where these viruses pose significant public health threats.

1. Introduction

Chikungunya virus (CHIKV) and dengue virus (DENV) are significant arboviruses affecting millions globally, with DENV alone impacting over 40 % of the global population annually, causing 50–100 million infections [1–3]. In 2023 alone, India reported approximately 150,000 cases of DENV, resulting in around 690 deaths due to severe manifestations of DENV, such as dengue hemorrhagic fever (DHF) and dengue shock syndrome (DSS). Although CHIKV cases were fewer in number compared to dengue and were associated with less mortality, they still pose a considerable health burden due to chronic incapacitating arthralgia persisting for years after the acute phase [4–6].

Both CHIKV and DENV have positive single-stranded RNA genomes (ssRNA+) that serve as mRNA, with viral proteins synthesized inside the host using host cellular machinery. Non-structural proteins aid in forming the replication complex, which initially generates a negative-strand viral RNA which is used as a template for transcribing multiple copies of new positive-strand viral genomes. Despite the morbidity and mortality associated with these infections, currently, only one FDA-approved vaccine exists for each virus (Ixchiq for CHIKV by Valneva

* Corresponding author. Centre for Immunobiology and Immunotherapy, Translational Health Science & Technology Institute (THSTI), 3rd Milestone, Faridabad-Gurgaon Expressway, Faridabad, Haryana, 121001, India.

** Corresponding author. Centre for Immunobiology and Immunotherapy, Translational Health Science & Technology Institute (THSTI), 3rd Milestone, Faridabad-Gurgaon Expressway, Faridabad, Haryana, 121001, India.

E-mail addresses: tanvi@thsti.res.in (T. Agrawal), aawasthi@thsti.res.in (A. Awasthi).

[1] These authors contributed equally.

https://doi.org/10.1016/j.bbrc.2024.150393
Received 23 May 2024; Received in revised form 5 July 2024; Accepted 10 July 2024
0006-291/

and Dengvaxia for DENV by Sanofi Pasteur) which are still not approved in India. Since no other approved targeted medical treatments such as antivirals exists till date, supportive measures become the mainstay of medical care. This highlights the urgent need for developing antivirals targeting CHIKV and DENV. Antivirals have the potential to shorten illness duration by inhibiting the virus, thereby improving clinical outcomes. Additionally, they could prove instrumental in managing outbreaks by halting the spread of infection from one person to another. Further, in view of the stigma associated with vaccines in many countries and cultures, antivirals can pave way for disease management.

Current trends in the pharmaceutical industry highlight a growing emphasis on exploring small molecules derived from natural sources as promising candidates for antiviral agents [7]. Recognizing the significance of natural compounds, we conducted a screening of 109 such compounds to evaluate their potential antiviral activity against CHIKV and subsequently on DENV. Among these compounds, we found lycorine, a phenanthridine alkaloid, isolated from plants of the Amaryllidaceae family [8] to be the most potent in inhibiting CHIKV and DENV. Previous studies exhibit diverse pharmacological effects of lycorine, including anticancer [9], anti-parasitic [10], anti-inflammatory [11,12] and antiviral effects with broad-spectrum inhibitory activity against various viruses, including poliovirus [13], severe acute respiratory syndrome-associated coronavirus (SARS-CoV) [14], SARS-CoV-2 [15], enteroviruses [16], members of Flaviviridae family such as hepatitis C virus (HCV) [17], Zika [18], DENV-2 [19] and West Nile virus [20], influenza virus [21] and CHIKV [22].

Although lycorine was already reported as an antiviral for both CHIKV and DENV-2, in this study we further wish to understand the exact mechanism of its action making it a strong antiviral against both viruses. We further wanted to see its effects on an Indian CHIKV strain belonging to the Indian Ocean Lineage (IOL) and on DENV serotypes 1–3 as this data was not available. In our investigation, we discovered that lycorine doesn't hinder viral entry for CHIKV but instead impedes the early stages of RNA replication. Furthermore, we demonstrated its potent inhibitory effect on all serotypes of DENV (DENV 1–4) and its ability to inhibit early DENV viral replication. Through in vitro and computational molecular docking studies, we elucidated that lycorine binds near the catalytic site of both CHIKV and DENV RNA Dependent RNA Polymerase (RdRp), exerting its action by inhibiting viral negative strand RNA synthesis, thereby effecting the viral RNA replication. In together, our findings indicate that lycorine is a potential candidate for the development of a broad-spectrum antiviral, especially targeting endemic arboviruses such as CHIKV and DENV in a resource-limited countries like India.

2. Materials and methods

2.1. Cell lines, viruses and reagents

In this study, Vero and Vero E6 cells (African green monkey kidney epithelial cells), Huh-7 cells (human hepatocellular carcinoma cells) and A549 cells (human pulmonary epithelial cells) were cultured in Dulbecco's Minimum Essential Medium (DMEM). C6/36 (*Aedes albopictus* mosquito cells) were cultured in Minimum Essential Medium (MEM) and THP-1 cells (human monocytic cells) were cultured in Roswell Park Memorial Institute (RPMI) medium. All cell growth media were supplemented with 10 % Fetal Bovine Serum (FBS), 100 U/ml penicillin, 100 μg/ml streptomycin, 1 % glutamine and C6/36 cells were supplemented with 1 % NEAA (Non-essential amino acids) additionally. The assay media used for infection, compound addition and cytotoxicity studies for all cell lines contained 2 % FBS besides above-mentioned additives. Vero, Vero E6, Huh-7, A549 and THP-1 cells were grown in a humidified incubator at 37 °C, whereas, C6/36 cells were kept at 28 °C with 5 % ambient CO_2. THP-1 monocytes were differentiated into macrophages by treatment with 30 ng/ml of PMA (Sigma, India) for 72 h. Post differentiation adherent cells were washed and used for further experiments. All cell culture reagents were purchased from Gibco (Thermo Fisher Scientific, India) and all cell lines were routinely checked for mycoplasma contamination.

Chikungunya virus Indian isolate strain (Ind-06-Guj, Gen Bank Accession No. JF274082) was a kind gift from Prof. Sudhanshu Vrati, Regional Centre for Biotechnology, Faridabad, India. DENV-1, DENV-2 and DENV-4 were obtained from BEI resources (NR-3785, NR-15247 and NR-48801 respectively). DENV-3 Indian clinical isolate (a kind gift from Dr. Gulam Hussain Syed, Institute of Life Sciences, Bhuvneshwar, India). Both chikungunya and DENV were propagated in C6/36 cells. Viral titers were determined by plaque-forming assay in Vero cells for CHIKV and by focus forming assay in Vero E6 cells for DENV [23]. Lycorine hydrochloride used in this study was purchased from Sigma, India while the natural compounds tested for initial screening were part of a natural product library from SelleckChem-L1400 (USA).

2.2. Plaque assay and focus forming assay

Plaque assay on Vero cells for CHIKV and focus forming assay on Vero E6 cells for DENV was used to determine the titers of all the supernatant and viral stocks. Briefly, 80,000 Vero cells per well/24 well plate and 20,000 Vero E6 cells per well/96 well plate were seeded. Virus was serially diluted 10-fold in DMEM assay media and cells were infected with serial dilutions of virus at 37°C, 5 % CO_2 for 1hr with intermittent rocking. Post-infection inoculum was removed and cells were overlaid with 0.5 % Carboxy Methylcellulose solution (CMC) (Sigma, India) prepared in DMEM assay media for CHIKV and 1.5 % CMC solution for DENV. The plates were incubated at 37°C under a humidified atmosphere of 5 % CO_2 for 26–28 h (hrs) for CHIKV and 48hrs for DENV. CMC solution was then aspirated and cells were fixed with 3.7 % formaldehyde solution for 30 min. For CHIKV formaldehyde solution was washed with tap water and cells were stained with crystal violet solution for 10 min followed by washing and air drying. Post-drying plaques were counted and titers were represented as Plaque Forming Unit (PFU)/ml. For DENV, the fixed cells were washed with PBS and were stained for DENV foci as the protocol given under section immunofluorescence. The DENV foci were counted using IX83 fluorescence microscope (Olympus) and titers were represented as Focus Forming Unit (FFU)/ml.

2.3. Virus inhibition assay

Vero cells were seeded in 96-well or 48-well plate (for CHIKV) and Vero E6 cells were seeded in 24-well plate for DENV to study the antiviral spectrum of lycorine by virus inhibition assays. The cells were infected with CHIKV at a multiplicity of infection (MOI) of 0.001 for Vero and A549 cells, 0.01 for C6/36 cells and MOI of 2 for Huh-7 and THP-1 macrophages. For DENV, cells were infected with a MOI of 0.1. Following infection for 1 h, viral inoculum was washed off and assay medium containing two-fold serially diluted lycorine starting from a concentration of 10 μM–0.078 μM for Inhibitory Concentration 50 (IC_{50}) determination or 5 μM for other experiments was added in triplicate wells. Control wells were treated with equal volume of Dimethyl Sulphoxide (DMSO) (Sigma, India) as vehicle control. After 18–24 h of incubation supernatant was collected from all wells for CHIKV and after 48 h for DENV. Viral titers in collected supernatants were measured by plaque assay for CHIKV and FFU assay for DENV. Inhibitory Concentration 50 (IC_{50}) was calculated in comparison to DMSO treated cells using GraphPad Prism Software.

2.4. Cytotoxicity assay

Cytotoxic effect of lycorine was tested on all cell lines. Cells were seeded in 96-well culture plates and treated with different concentrations of lycorine (50 μM, 25 μM, 10 μM, 5 μM, 1 μM and 0.5 μM). The control wells were treated with an equal volume of DMSO. After 24 h, cell viability was assessed by formation of formazan crystals by MTT [3-(4,5- dimethylthiazol-2-yl) 2,5diphenyltetrazolium bromide] reagent (Sigma, India). 10 % MTT reagent (5 mg/ml) in serum free media was added to each well and the plate was incubated for additional 4 h at 37°C with 5 % CO_2. After incubation MTT containing media was removed and the crystals were dissolved in DMSO. The absorbance values were measured at 590 nm and percentage cytotoxicity was calculated with respect to DMSO treated cells. Cytotoxic Concentration 50 (CC_{50}) was calculated using GraphPad Prism Software v8.0.

2.5. Time of addition/removal assay

Vero cells were seeded in 24-well plate overnight, and then infected with CHIKV at an MOI of 0.1. Lycorine was added to one set of triplicate wells 2 h prior to virus infection to study if lycorine modulates entry receptors on cells and was removed before infection of cells. For 0–1 h time, lycorine was added during infection (0–1 h), and was removed when virus inoculum was removed from the cells with no lycorine added to post infection media. To the rest of wells lycorine was added at 0, 2, 4, 6, 8 and 10 h post infection (hpi) (Fig. 3A). The control wells were treated with an equal volume of DMSO. After 18 hpi, supernatant was collected and viral titers were determined by plaque assay.

2.6. Immunofluorescence

Vero and Vero E6 cells were grown in a 24-well plate and were infected with 0.001 MOI CHIKV and 0.1 MOI of DENV respectively. Post-infection lycorine was added at various concentrations. Eighteen hours post-infection for CHIKV and 48 h post infection for DENV, cells were fixed with 4 % paraformaldehyde solution for 20 min at Room Temperature (RT). Cells were washed twice with PBS and cell membranes were permeabilized with PBS containing 0.1 % Triton X-100 for 15 min. Non-specific antibody binding sites were blocked by incubating with PBS containing 1 % Bovine Serum Albumin (BSA) for 1 h at RT. The cells were then incubated with the following primary antibodies; In-house generated mouse antibody binding to CHIKV envelope protein (CHK-263) and anti-DENV primary antibody (Mab8705, Millipore). Cells were incubated in primary antibodies for 1 h at RT, washed thrice with PBS and incubated with anti-mouse secondary antibody conjugated with Alexa-flour 488 for 1 h at RT. Nuclei were stained by Hoechst stain (1:500 dilution in PBS) for 5 min for CHIKV experiments and washed twice with PBS. All images were acquired using IX83 fluorescence microscope (Olympus).

2.7. RNA isolation and qRT-PCR

Vero or Vero E6 cells were infected with CHIKV and DENV-2 respectively and cells were collected at indicated time points. Total cellular RNA was isolated using Trizol reagent (Thermo Fisher Scientific, India) and around 500 ng RNA was reverse transcribed using the Verso cDNA reverse transcription kit (Thermo Fisher Scientific, India) using random hexamers as follows: 42°C for 30 min followed by inactivation at 95 °C for 2 min. Briefly, 50 ng of cDNA was used as a template for quantitative reverse transcription-polymerase chain reaction (qRT-PCR) to target conserved region of the NSP3 gene for CHIKV (NSP3; FP: 5′-GCGCGTAAGTCCAAGGGAAT-3′, RP: 5′-AGCATCCAGGTCTGACGGG-3′) [24] and NS5 for DENV (NS5; FP: 5′-GGTTAGAGGAGACCCCTC-3′, RP: 5′- GAGACAGCAGGATCTCTG -3′) [23]. The GAPDH mRNA levels (glyceraldehyde-3-phosphate dehydrogenase) were determined in parallel in all samples and used as an endogenous control for normalization through qRT-PCR. The primer sequences for GAPDH detection in Vero cells and human cells were as follows: (Vero GAPDH; FP: 5′-ATTCCACCCATGGCAAATTC-3′, RP: 5′-CGCTCCTGGAAGATGGTGAT-3’; Human GAPDH; FP: 5′-GAAATCCCATCACCATCTTCCAGG-3′, RP: 5′-GAGCCCCAGCCTTCTCCATG-3′). The qRT-PCR reaction mixture contained final concentrations of primers at 200 nM and the samples were run in duplicates. The assay was performed with an Applied Biosystems 7500 RT-PCR systems (Life Technologies, USA) with 2 × Power SYBR Green PCR Master Mix (Thermo Fisher Scientific, India), following the manufacturer's protocol. PCR cycling parameters were 95 °C for 10 min, followed by 40 cycles of 95 °C for 15 s and 60 °C for 1 min. Relative expression in levels of viral RNA in lycorine treated and DMSO treated cells at various time points were calculated using comparative threshold cycle method. For detection of negative strand CHIKV and DENV RNA, cDNA synthesis was performed using the forward primers used in qRT-PCR. Fold change in expression of negative strand RNA was quantified as described above.

2.8. RNA-dependent RNA polymerase (RdRp) proteins and structure preparations

We selected the DENV-2 RdRp co-crystal (PDB-id: 5K5M, HOLO, 2.01 Å resolution) for our study due to its high resolution. Another similar structure (PDB-id: 6IZY, APO, 2.11 Å resolution) was compared using Maestro's Protein Structure Alignment tool, showing a RMSD of 1.21 Å. The better resolution of 5K5M made it our choice for further DENV studies. For CHIKV RdRp, we used the best-resolved Alphavirus structure available, i.e for Sindbis virus (SINV) (PDB-id: 7VB4, Chain B, APO) due to the lack of CHIKV RdRp crystal structure (Fig. S7).

Both protein structures were optimized using Maestro's Protein Preparation Wizard. Missing regions were interpolated, hydrogens added with correct stereochemistry, and ionization states maintained at pH 7.0. Missing side-chain atoms were added using the Xiang and Honig rotamer library, with subsequent optimization focusing on maximizing hydrogen bonding. Freely rotating hydrogens, protonation states of charged residues, tautomers of His residues, and Chi 'flip' for Asn, Gln, and His residues were all considered [25]. Energy minimization with the OPLS4 force field was conducted until heavy-atom displacement reached an RMSD of 0.30 Å. The catalytic domains of DENV-2 and SINV RdRps feature a hand-like architecture with finger, palm, and thumb regions, crucial for catalytic activity [Fig. S7]. Detailed residue information for these domains was extracted from previous studies [26,27].

2.9. Binding site mapping

Lycorine's docked poses were matched with 19 known DENV-RdRp co-crystal structures (PDB-ids: 5K5M, 6IZX, 6H80, 3VWS, 5IQ6, 5HMX, 5F3Z, 5HMY, 5HN0, 5I3P, 5F3T, 5HMZ, 6XD0, 5F41, 5I3Q, 6XD1, 2J7W, 5HMW, 61ZZ) from the RCSB PDB databank to mine residue-specific information. For SINV, RdRp structure (7VB4) was used due to limited crystallographic data.

2.10. Drug preparation, ligand selection and preparation

Lycorine's 2D structure was drawn and its 3D structure developed in Maestro for molecular docking studies with DENV-2 and SINV co-crystal structures. Ligands were prepared using Schrödinger's LIGPREP (2017-1) and optimized with the OPLS3 force field [28]. Both binding site-specific (ligand-independent) and drug-specific (ligand-dependent) methods were used to identify Lycorine's binding sites in DENV and SINV RdRps.

2.11. Molecular docking

Docking studies (ligand-dependent) were conducted using AUTODOCK4.2 [29] and GLIDE to identify Lycorine's potential binding sites and its therapeutic efficacy against both RdRps. Both tools were used to explore predicted binding sites, selecting the most consistent ones based on lowest docking energies and cluster size. Blind Docking (BD) was initially performed with the entire protein as the grid, followed by Focused Docking (FD) to refine and optimize binding poses.

2.12. SiteMap analysis

SiteMap analysis (ligand-independent) was performed to predict potential binding sites on crystals 5K5M and 7VB4 using the Schrodinger Suite's SiteMap program [30]. This unbiased method calculates the druggability of identified sites, employing the OPLS-2005 force field with a standard grid of 15 site points per reported site, cropped at 4.0 Å from the nearest site point.

2.13. Free energy analysis through MM-GBSA (Molecular Mechanics/Generalized Born Surface Area)

Binding energy was calculated using MM-GBSA (Prime module of Maestro) with the formula ΔGbind = ΔEMM + ΔGsolv + ΔGSA. Here, ΔEMM represents the minimized energy difference between ligand and protein complexes, ΔGsolv is the GBSA solvation energy difference, and ΔGSA accounts for surface area energy differences between the complex and individual components [31].

2.14. Statistical Analysis

All the results were analysed and plotted using GraphPad Prism 8.0 software. For direct comparisons between two groups, Student's unpaired *t*-test was used, and for multiple comparisons between more than two groups, 1- or 2-way ANOVA was performed to determine between-groups statistical significance, where $*p < 0.05$, $**p < 0.01$, $***p < 0.001$, and $****p < 0.0001$ were considered significant.

3. Results

3.1. Lycorine inhibits CHIKV infection in Vero cells

In order to identify antivirals against CHIKV, we screened 109 natural compounds from a commercial library from SelleckChem, USA in Vero cells for their ability to inhibit CHIKV infection (Fig. S1) and found lycorine to be the most effective (Fig. S1). Lycorine (Fig. 1A), at a concentration of 5 μM exhibited potent inhibitory activity against CHIKV with a 4 $\log_{10}$ reduction in viral titers in culture supernatants compared to DMSO treated cells (Fig. 1B). Lycorine further showed inhibition of CHIKV in a dose-dependent manner with an IC_{50} of 0.319 μM (Fig. 1C). To check whether this decrease in virus is not due to direct cytotoxicity of lycorine on cells, MTT assay was performed and the CC_{50} was found to be > 50 μM making the Selectivity Index (SI, CC_{50}/IC_{50}) on lycorine on Vero cells to be > 156 (Fig. 1E). This suggests that lycorine was not toxic to cells at lower concentrations. To further analyse whether the reduction in CHIKV titers was due to inhibition of viral RNA or inhibition in production of viral proteins, qRT-PCR for viral RNA and immunofluorescence targeting CHIKV envelope protein were performed. qRT-PCR analysis of 5 μM lycorine treated cells showed around 3.5–4 $\log_{10}$ fold reduction in CHIKV viral RNA as compared to DMSO treated cells (Fig. 1C) while immunofluorescence showed complete inhibition of viral protein even at 2.5 μM concentration of lycorine (Fig. 1F). These results suggest that inhibition of CHIKV titers is not due to inhibition of viral protein synthesis but rather due to inhibition of viral replication.

3.2. Lycorine inhibits CHIKV infection independent of cell type

To order to investigate whether lycorine can inhibit CHIKV independent of cell type, we tested the inhibitory effect of lycorine on different cells lines comprising both human and mosquito cells. Huh-7 cells, A549 cells and THP-1 macrophages were infected with CHIKV and treated with lycorine at different concentrations. Similar to Vero cells, lycorine inhibited CHIKV viral titers in supernatants in all three human cell lines in dose-dependent manner with similar IC_{50} as found in Vero cells [Huh-7 IC_{50} – 0.214 μM; A549 IC_{50} – 0.306 μM and THP-1 macrophages IC_{50} – 0.307 μM] (Fig. 2A). In all the human cell lines tested, lycorine exhibited minimal cytotoxicity with CC_{50} equal to or more than 50 μM (Fig. 2B) making the SI for all three human cells lines >160. Similar to all the cell lines tested previously, an equivalent inhibitory effect of lycorine was further observed in mosquito cell line C6/36 infected with CHIKV (IC_{50} – 0.366 μM). The cytotoxicity of lycorine was however more in C6/36 with a CC_{50} of 8.8 μM. Our results thus suggests a more direct virus acting mechanism of lycorine rather than involvement of host proteins.

3.3. Lycorine inhibits early stage of CHIKV viral replication

In order to understand the step in viral life cycle at which lycorine acts, a time of addition/removal assay was performed. Vero cells were infected with CHIKV and at indicated time points (Fig. 3A), lycorine was added and/or removed to the cells pre or post-infection at a concentration of 5 μM. To study if lycorine modulates entry receptors on cells, lycorine was added 2 h prior to infection (-2 h time point) and was removed before infection of cells. To study if lycorine inhibits viral entry to cells by directly acting on virus, lycorine was added during infection (0–1 h), and was removed when virus inoculum was removed from the cells with no lycorine added to post infection media. The time point of 0 h indicates that lycorine was added along with the addition of virus similar to 0–1 h time point but post infection media also contained lycorine. Viral titers in all sets were measured in supernatants collected at 12 hpi. It was observed that pre-treatment of lycorine (-2 h) or treatment during infection alone (viral adsorption step; 0–1 h) does not inhibit viral titers, suggesting that lycorine does not block viral entry (Fig. 3B). Maximum inhibition was seen when lycorine was added just at the start of infection (0 h) followed by addition after 2 h to cells. We further observed that lycorine exerted its inhibitory effect even when added till 10 hpi. These results show that lycorine inhibits early stages of viral replication.

3.4. Lycorine inhibits dengue infection

DENV, a flavivirus, is another endemic arboviral infection in India with significant burden on public health. Lycorine has been previously shown to inhibit DENV-2 and other Flaviviridae members like Zika and HCV [11,22]. In this study, we tested the antiviral activity of lycorine against all serotypes of DENV. Vero E6 cells were infected with DENV 1–4 and post infection various concentrations of lycorine were added to cells as shown in Fig. 4. Supernatants were collected from infected cells at 48hpi and were subjected to FFU assay for determination of IC_{50}. The cells after collection of supernatants were fixed and subjected to immunofluorescence using an anti-Dengue envelope protein antibody. Our results show that lycorine inhibited all four serotypes of DENV in a dose dependent manner. All serotypes showed a 50 % inhibition in DENV virus between a lycorine concentration of 0.59–0.48 μM (Fig. S2) suggesting that lycorine inhibits DENV also at low micromolar concentrations.

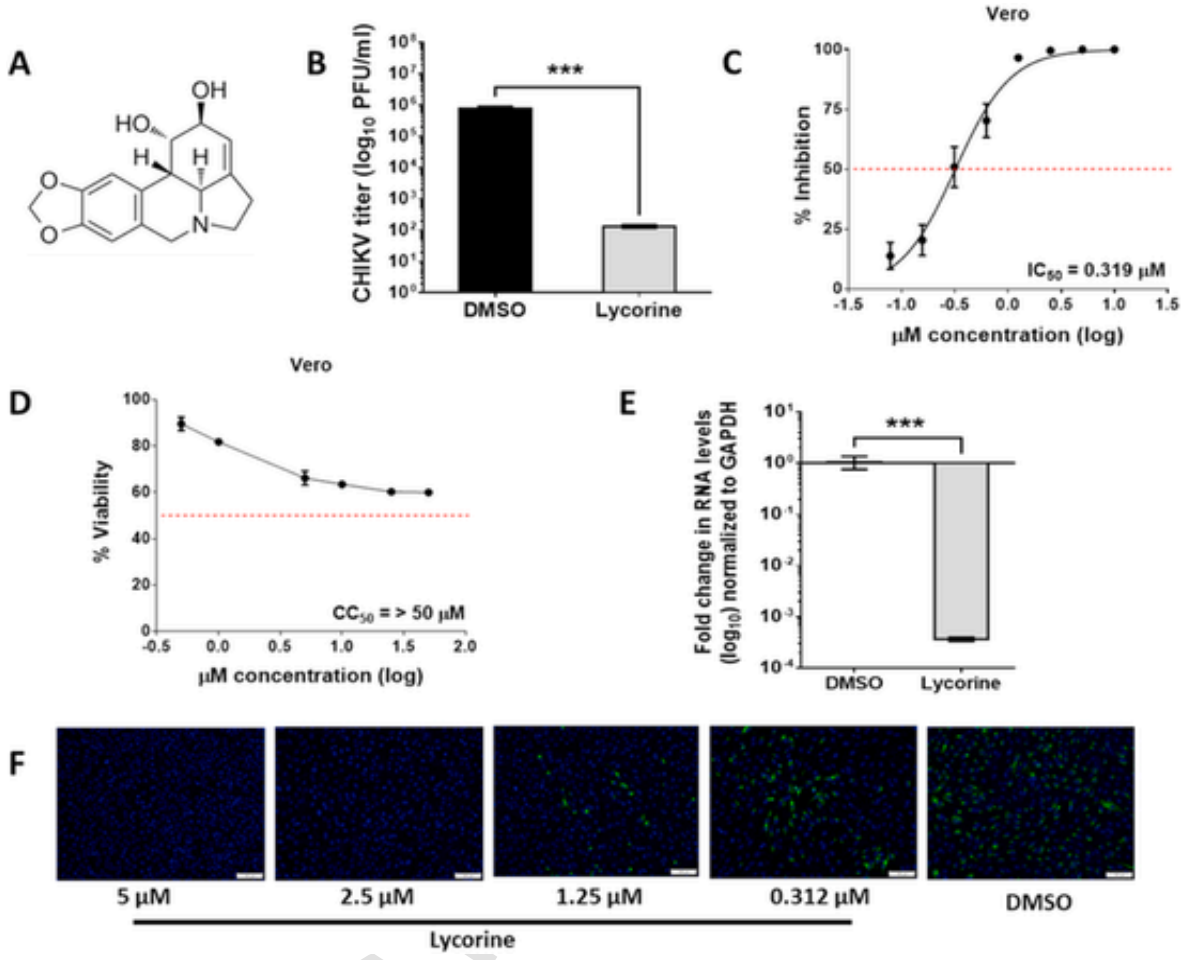

Fig. 1. Lycorine inhibits CHIKV in Vero cells. (A) Chemical structure of lycorine. (B) CHIKV titers expressed as log_{10} PFU/ml in lycorine and DMSO treated cells. Vero cells were infected with CHIKV and treated with either 5 µM lycorine or equal amount of DMSO post-infection. At 18 hpi supernatant for plaque assay and cells for RNA isolation and qRT-PCR were collected. (C) IC_{50} and (D) CC_{50} determination for lycorine in Vero Cells. Vero cells were infected with CHIKV and lycorine was added to cells at various concentrations (10 µM–0.078 µM for IC_{50}). Equal volume of DMSO was added to control wells. Viral titers were measured in supernatant and % inhibition in comparison to DMSO treated cells was calculated. Cell viability in comparison to DMSO treated cells was assessed by MTT assay. Lycorine was added to cells in various concentrations (50 µM–0.5 µM) and MTT assay was performed after 24 h and CC_{50} was calculated. (E) Log_{10} fold change in expression of CHIKV viral RNA. The expression of viral RNA in DMSO treated cells was taken as 1 and comparative fold change in lycorine treated cells was analysed. GAPDH expression was used to normalise results. (F) The antiviral activity of lycorine against CHIKV was determined by an immunofluorescence assay. Cell nuclei were stained with Hoechst (blue). Envelope protein was immune-stained with an anti-CHIKV envelope antibody (CHK-263). The envelope protein is indicated in green. All experiments were repeated twice and figures are represented from one experiment. Scale bar for (F): 100 µm. Figures are representative of two or more experiments done in triplicates. Error bars indicate mean ± SD. ***$p < 0.0001$ as determined by two-tailed *t*-test. (For interpretation of the references to color in this figure legend, the reader is referred to the Web version of this article.)

3.5. Lycorine inhibits viral RNA replication at the stage of negative strand synthesis

For CHIKV, the above results suggested that lycorine probably inhibited early stages of viral replication. To further substantiate these results, we analysed viral RNA dynamics at various time points for both CHIKV and DENV-2 through qRT-PCR. Cells were infected with CHIKV and DENV-2 and post-infection, 5 µM lycorine was added to cells. The cellular RNA was isolated at indicated time points and subjected to qRT-PCR. Both CHIKV and DENV-2 viral RNA showed significant reduction in lycorine treated cells compared to DMSO treated cells (Fig. 5A and B). In case of CHIKV, fold change in the level of viral RNA expression was around 2 log_{10} less at 4 hpi and 2.5–3 log_{10} less at 8 hpi, in lycorine treated cells as compared to DMSO treated cells. (Fig. 5A). For DENV-2 also, by 24 hpi there was a 2.5 log_{10} fold reduction in viral RNA in lycorine treated cell compared to DMSO treated cells (Fig. 5B). To understand the stage at which RNA replication is affected by lycorine, we further studied the fold changes in expression of negative strand viral RNA in lycorine treated cells. For CHIKV, which has a fast replication cycle in Vero cells and the expression of negative strand RNA starts as early as 1 hpi [32] we observed that at 2 hpi, the fold change in expression of negative strand RNA was around 2 times less in lycorine treated cells and by 4 hpi it was further reduced by more than 10-fold suggesting an inhibition in negative strand RNA synthesis (Fig. 5C). Since flavivirus RNA replication starts late mostly after 5 hpi to 6 hpi [33], the negative strand RNA levels were measured for DENV-2 at 6 hpi, 10 hpi and 16 hpi. The negative strand RNA levels were similar in lycorine treated and DMSO treated cells at 6 hpi but a 30-fold reduction was observed at 10 hpi (Fig. 5D). Furthermore, we observed that in CHIKV, the negative strand RNA levels in lycorine treated cells at 4 hpi increase by 4 folds as compared to 2 hpi, however, we were not able to explain the reason and the data needs further elucidation. Our overall results along with the time of addition assays suggest that lycorine in-

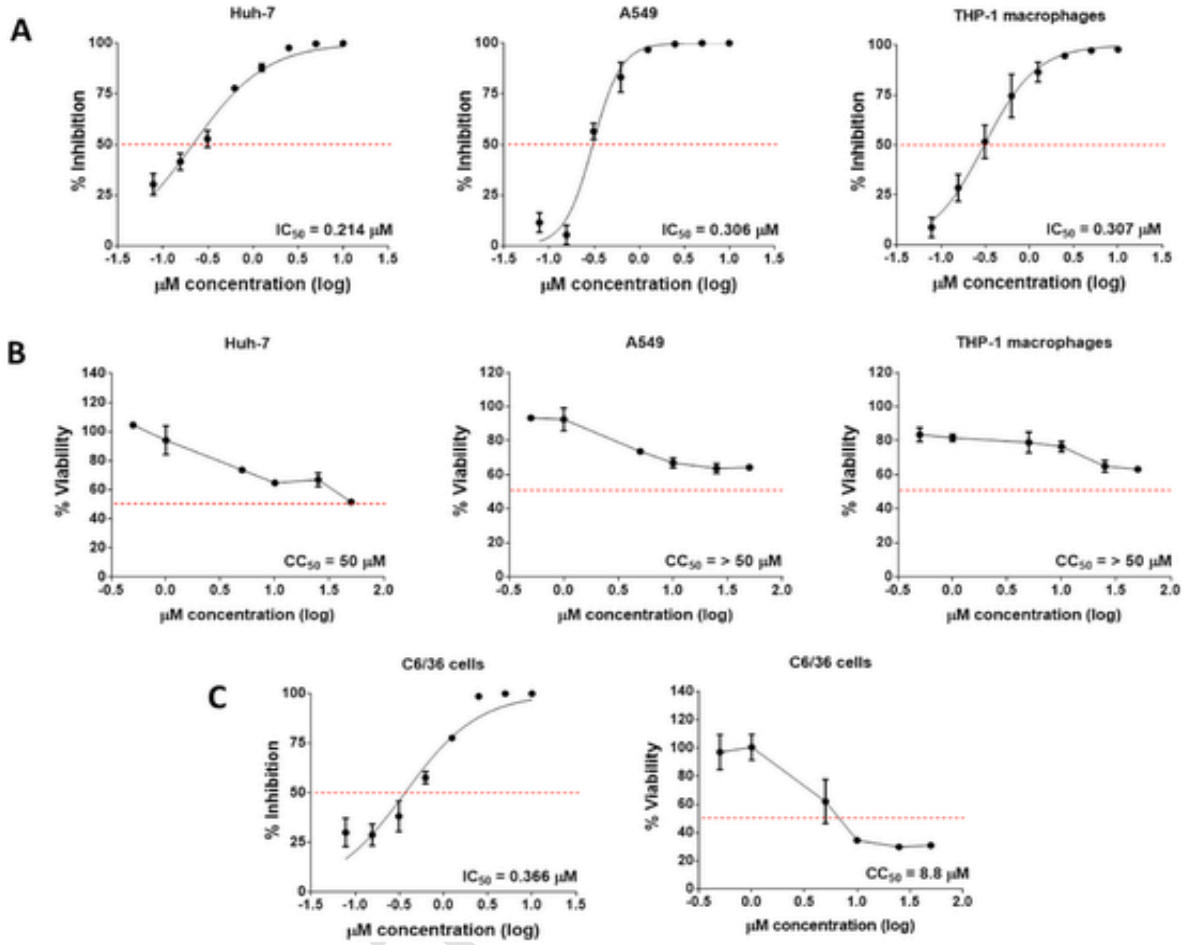

Fig. 2. Lycorine inhibits viral replication in many cell types. (A) IC_{50} for lycorine in Huh-7, A549 and THP-1 macrophages. Huh-7, A549 and THP-1 macrophages were infected with CHIKV and lycorine was added to cells at various concentrations (10 μM–0.078 μM). Equal volume of DMSO was added to control wells. Viral titers were measured in supernatant and % inhibition in comparison to DMSO treated cells was calculated. (B) CC_{50} for lycorine in Huh-7, A549 and THP-1 macrophages. Cell viability in comparison to DMSO treated cells was assessed by MTT assay. Lycorine was added to cells in various concentrations (50 μM–0.5 μM) and MTT assay was performed after 24 h and CC_{50} was calculated. (C) IC_{50} and CC_{50} for lycorine in C6/36 mosquito cells. Figures are representative of two or more experiments done in triplicates.

hibits negative strand synthesis, thereby subsequently preventing positive strand RNA synthesis and thus viral replication.

3.6. RdRp structure preparation and molecular docking

Lycorine's binding activity to SINV and DENV RdRps was evaluated using molecular docking, building on its known inhibition of Zika virus RdRp, a member of the Flavivirus family. Protein Structure Alignment in Maestro revealed a RMSD of 4.62 Å between the RdRps, indicating structural differences that could affect Lycorine's binding sites.

Due to limited co-crystals for DENV-2 RdRp, other serotype co-crystals were included. Among the 19 DENV co-crystals, binding sites were found near the Finger domain (6XD1, 6XD0, 5IQ6, 7VWS), the Thumb domain (6IZZ, 6IZX, 5HMX, 5HMW), and the Thumb-Palm junction (6H80, 5I3Q, 5I3P, 5HN0, 5HMZ, 5HMY, 2J7W, 5F41, 5F3Z, 5F3T).

Initial Blind Docking (BD) identified conformers with large cluster sizes and lowest binding energies (LBE). For SINV, the best sites were S1 (−6.2 kcal/mol, cluster size: 92), S2 (−6.9 kcal/mol, cluster size: 10), and S3 (−6.3 kcal/mol, cluster size: 15) (Fig. 6A and Fig. S4). For DENV-2, the best sites were S1 (−6.25 kcal/mol, cluster size: 30), S2 (−6.52 kcal/mol, cluster size: 30), and S3 (−6.18 kcal/mol, cluster size: 11) (Fig. 6B and Fig. S5).

Overall view of the SINV RdRp and DENV-2 RdRp with the same orientation and colour coding as in Fig. S7 with the RdRp rendered in Transparent Material for better visualization. The active sites (S) with higher conformations as well as docking energies are boxed on each RdRp. The lycorine structures are displayed in licorice. (A) On SINV RdRp, 3 best sites with higher conformations and docking energies are represented as S1 in magenta (color), S2 in red (color) and S3 in green (color). (B) On DENV-2 RdRp, 3 best sites with higher conformations and docking energies are represented as S1 in ochre (color), S2 in pink (color), and S3 in yellow (color).

3.7. SiteMap Analysis

SiteMap analysis (ligand-independent) confirmed the predicted binding regions on structurally minimized RdRps. Sites 1 and 2 overlapped well for both SINV and DENV-2, but S3 in SINV was not recognized by SiteMap. Despite this, S3 was considered due to its low docking energy. The best druggability scores (D-score) were 1.067 for 5K5M and 0.973 for SINV, with pocket sizes of 220 and 218, respectively (Fig. S3).

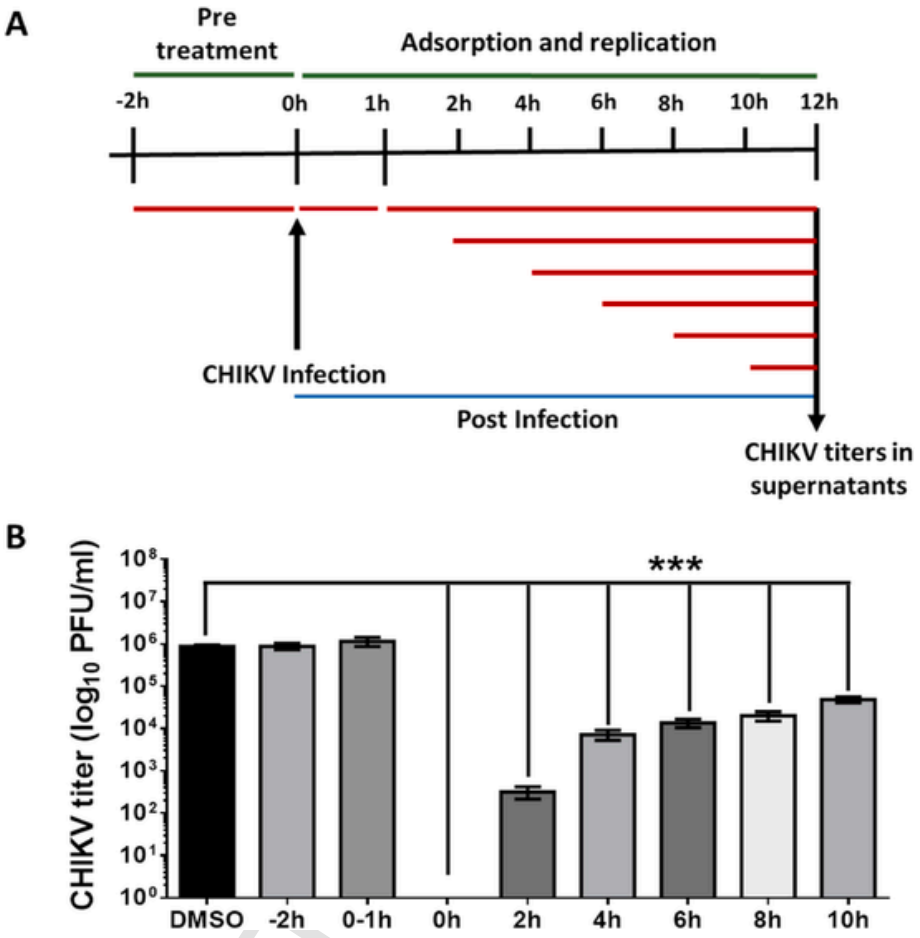

Fig. 3. Time of addition assay. (A) Schematic representation of time points at which lycorine was added, pre-infection (−2 h), during infection (0–1 h) and post infection (0 h, 2 h, 4 h, 6 h, 8 h and 10 h). Vero cells were infected with CHIKV and at various time point pre-infection and post-infection, 5 μM lycorine was added. Viral titers in supernatants were measured at 12 hpi. (B) CHIKV titers expressed as log_{10} PFU/ml in cells treated at indicated time points. Figures are representative of two or more experiments done in triplicates. Error bars indicate mean ± SD. ***p < 0.0001 as determined by two-tailed *t*-test.

3.8. Free Energy Analysis (MM-GBSA)

MM-GBSA binding free energy calculations further assessed site stability. For 5K5M, the order was S3 (−67.28 kcal/mol) > S2 (−46.29 kcal/mol) > S1 (−33.17 kcal/mol) (Fig. 6B). For 7VB4, it was S3 (−52.55 kcal/mol) > S1 (−38.92 kcal/mol) > S2 (−25.08 kcal/mol). Thus, S2 and S3 in DENV-2, and S1 and S3 in SINV were considered potential binding sites (Fig. 6A).

3.9. Focused Docking (FD)

FD was performed at the selected sites, revealing dynamic shifts in LBE: DENV-2 S3 (−6.18/-6.61) and SINV S1 (−6.2/-8.98) and S3 (−6.3/-7.75). The results suggest S3 in DENV-2 and either S1 or S3 in SINV as potential binding sites (Figs. S4 and S5).

3.10. Final Analysis and Conclusion

To confirm the most likely binding sites in case of DENV-2, we superimposed the identified S1, S2 and S3 representatives over 19 co-crystals of DENV RdRp. Other than docking and MM-GBSA energy the other reason of selection of these binding sites are their vicinity with reported co-crystals. The S1 and S2 are in vicinity with 3VWS (ligand VWS), and 5IQ6 (ligand 6CJ), respectively (Fig. S6). However, the best overlap has been shown by S3 with 3VWS, suggesting S3 seems the most likely Lycorine's binding site. For SINV, S1 was preferred due to its SiteMap alignment, MM-GBSA score, and BD/FD LBE performance despite S3's higher MM-GBSA score. Therefore, S1 is proposed as Lycorine's binding site for SINV RdRp. Moreover, it was observed that the lycorine binding site appears different in both RdRps.

3.11. Binding site characterization, S1: SINV and S3: dengue

Based on interaction fingerprinting at the potential binding site, (i.e. Site 1 in SINV RdRp), hydrogen bonds (HBs) were formed by Lycorine with residues GLU368 (3.06 Å), ASP466 (1.52 Å and 3.14 Å), LYS526 (2.79 Å), and ARG572 (1.95 Å) (Fig. 7A). Additionally, 2 hydrophobic interactions with VAL186 (3.84 Å) and TYR503 (3.74 Å) were also observed which strengthen the binding affinity. Two salt bridges were also noticed featuring ASP370 (4.41 Å) and ASP466 (4.72 Å) are also contributing (Fig. 7A). The S1 binding site in case of SINV is also encompassed by the active binding site within the palm domain lying with residues Asp466 and Asp371, crucial for catalytic activity [27] indicating these are critical determinants to consider S1 as the most likely binding site.

In DENV-2 RdRp at site S3, hydrogen bonds were formed with residues LEU409 (2.13 Å and 3.07 Å), MET477 (3.06 Å), and ARG482 (2.08 Å, 3.37 Å, and 2.21 Å) (Fig. 7B). These HBs are dynamic with different atoms of same amino acids. Additionally, a total of 2 hydrophobic interactions were observed with ALA411 (3.85 Å) and ILE474

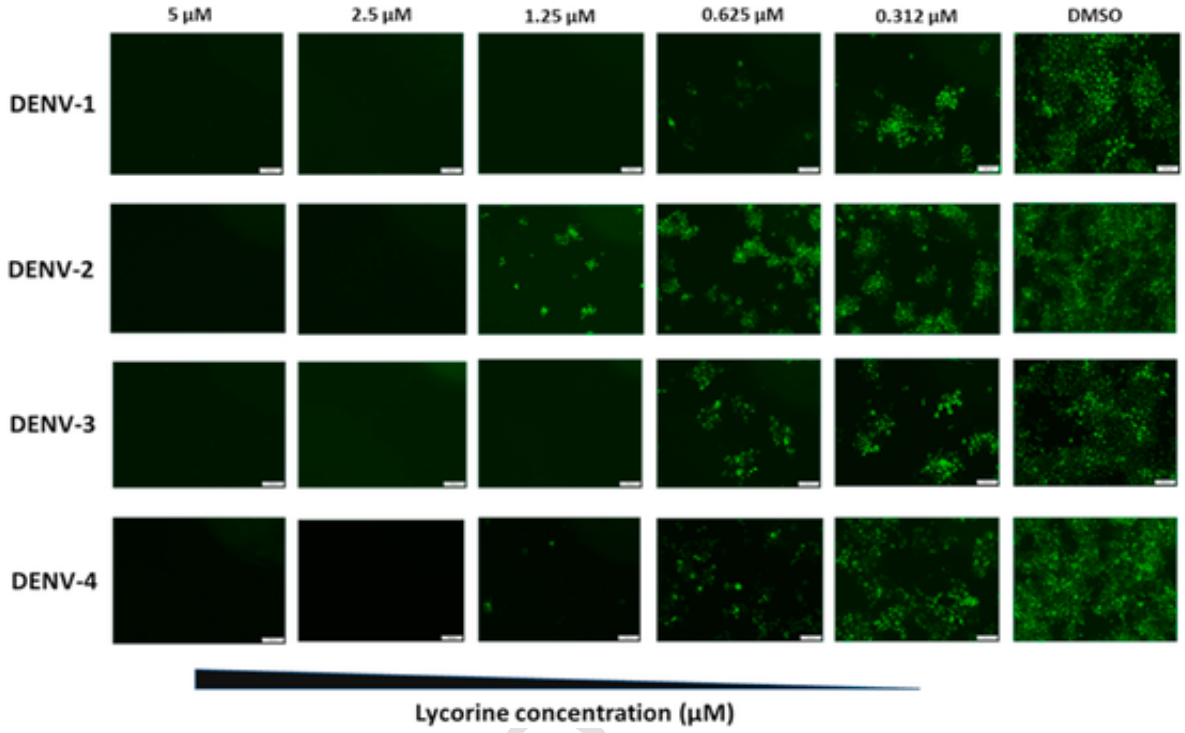

Fig. 4. Lycorine inhibits Dengue viral replication. Vero E6 cells were infected with DENV 1–4 and various concentrations of lycorine were added post-infection (5 μM, 2.5 μM, 1.25 μM, 0.625 μM, and 0.312 μM). The antiviral activity of lycorine against DENV was determined by an immunofluorescence assay. DENV envelope protein was immune-stained with a commercial anti-DENV envelope monoclonal antibody. The envelope protein is indicated in green. All experiments were repeated twice and figures are represented from one experiment. Scale bar: 100 μm. (For interpretation of the references to color in this figure legend, the reader is referred to the Web version of this article.)

(3.41 Å). Considering the strong binding affinity and a nice overlap with co-crystal, The S3 seems the most likely lycorine binding site in DENV-2.

Detailed view of proposed lycorine binding site, with residues from (A) SINV RdRp and (B) DENV-2 RdRp participating in the interaction and coloured using the same colour coding as in Fig. 6. Protein RdRp are rendered in new cartoons and lycorine is licorice in atom-wise mode, C: yellow (S3 in DENV2 RdRp) and magenta (S1 in SINV RdRp), H:black, N:blue, O:red and S:yellow.

4. Discussion

Our study commenced with the aim of identifying a natural compound that could inhibit CHIKV infection. We tested 109 natural compounds at a concentration of 5 μM to pinpoint those capable of inhibiting CHIKV at low micromolar levels. Among these, lycorine emerged as the most potent inhibitor. Lycorine has been previously shown to inhibit multiple viruses, including CHIKV [22] and DENV-2 [19]. For CHIKV, the study conducted by Li et al. [22] utilized the WT strain from China (CHIKV-JC2012), an Asian strain, whereas we sought to examine the impact of lycorine on an Indian clinical isolate belonging to the Indian Ocean lineage which exhibited higher replicative capacity. This was evident as Li et al. employed a high MOI of virus (MOI of 10) for their time of addition assays, but when we used a MOI of 1 for our time of addition experiments it led to complete cell death by 10 hpi in DMSO treated cells. This reflects that the strain we used may have higher replicative capacity as compared to the Asian strain. In time of addition studies done by Li et al., despite using a concentration of 10 μM lycorine, they found virus in supernatant when lycorine was added concurrently with the virus addition to cells (0 h time point of our assay). However, we found complete inhibition of CHIKV when lycorine (5 μM) was added concurrently with the virus (0 h time point). This suggests that lycorine's efficacy in inhibiting CHIKV at very stages of viral replication cycle depends on strain used.

Since compound activity can vary depending on cell type, it's crucial for an antiviral candidate for viruses infecting humans to exhibit considerable activity in human cells as well. We, thus assessed lycorine's impact on CHIKV inhibition using three human cell lines: Huh-7 (liver), A549 (lung), and THP-1 macrophages (immune). THP-1 macrophages were chosen due to their documented involvement in CHIKV pathogenesis [34,35] and it would showcase lycorine as an effective antiviral drug if it inhibits CHIKV in macrophages. The IC_{50} results obtained in all three human cell lines were consistent with those in Vero cells (primate cells). Additionally, when examined for its inhibitory activity in C6/36 mosquito cells, lycorine displayed inhibition of CHIKV at low micromolar concentrations (IC_{50} – 0.366 μM) in mosquito cells also. These findings indicate that lycorine 's inhibition of CHIKV is not influenced by cell type or organism, but rather direct targeting of a viral protein.

In India, both CHIKV and DENV are major vector-borne viral diseases transmitted by *Aedes aegypti* and *Aedes Albopictus,* posing a serious public health risk. Consequently, we conducted a further analysis of lycorine's inhibitory impact on DENV. While some earlier studies have reported lycorine's inhibitory effects on DENV-2 [19], none of them examined its effects on all four DENV serotypes (DENV 1–4). Our results show inhibition of all four DENV serotypes by lycorine in low micromolar concentrations suggesting that lycorine inhibits both CHIKV and DENV.

Our time-of-addition assay unequivocally indicated that lycorine does not hinder viral entry or exit but rather targeted an early stage of viral replication. This is evident from the fact that maximum effect of lycorine (no plaques observed in supernatant), was observed when it

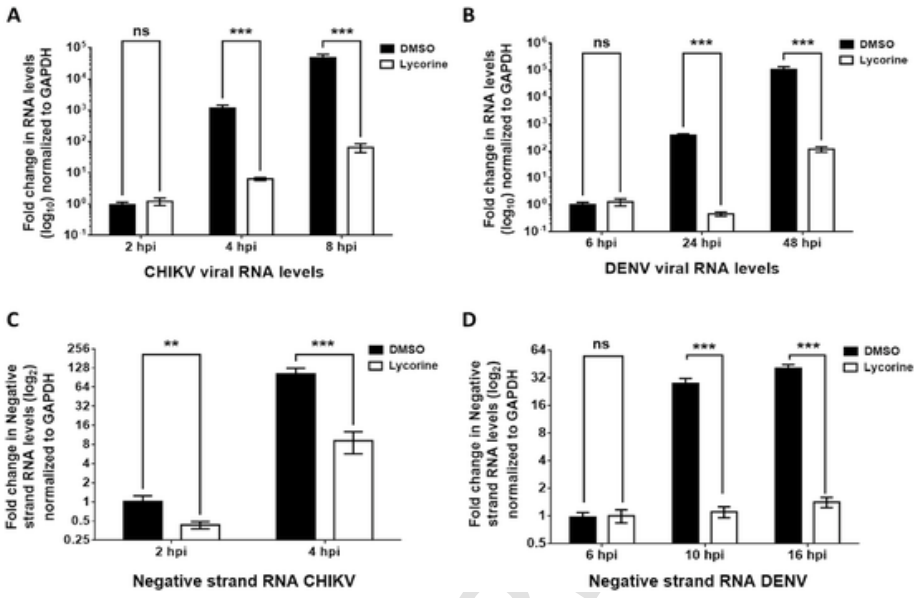

Fig. 5. Viral RNA dynamics in lycorine treated cells. (A) Log_{10} fold change in expression of CHIKV viral RNA and (B) Log_{10} fold change in expression of DENV-2 viral RNA. Vero cells were infected with CHIKV and Vero E6 cells were infected with DENV-2. Post-infection 5 μM lycorine was added. DMSO treated cells were taken as controls. At indicated time points (2 h, 4 h and 8 h for CHIKV and 6 h, 24 h and 48 h for DENV) cells were collected, RNA was isolated and viral gene expression was studied by qRT-PCR. (C) Log_2 fold change in expression of CHIKV negative strand viral RNA and (D) Log_2 fold change in expression of DENV-2 negative strand viral RNA. For negative strand viral expression, cDNA synthesis was done with the forward primer used for qPCR and the product was analysed through qPCR. For analysing the fold change in expression of both positive and negative strand viral RNA, the fold expression in DMSO treated cells at 2 h for CHIKV and at 6 h for DENV was taken as 1 and comparative fold change in lycorine and DMSO treated cells at all time points were analysed in comparison. GAPDH expression was used to normalise results. Figures are representative of two or more experiments done in triplicates. Error bars indicate mean ± SD. $^{**}p < 0.001$ and $^{***}p < 0.0001$ as determined by one-way ANOVA.

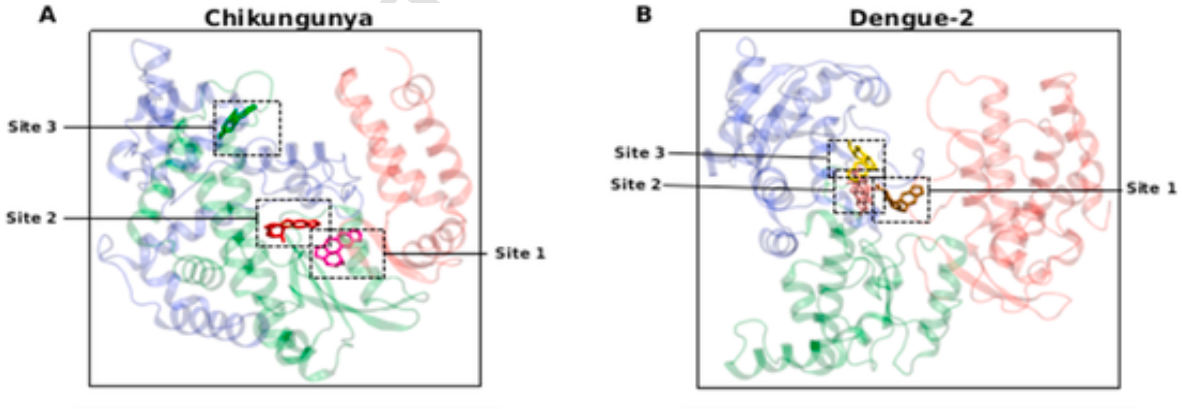

CHIKV RdRp best poses (docking results)			
Site (S)	Blind	Focused	MMGBSA
S1	-6.2/92	-8.98/179	-38.92
S2	-6.9/10	-7.87/200	-25.08
S3	-6.3/15	-7.75/172	-52.55

DENV-2 RdRp best poses (docking results)			
Site (S)	Blind	Focused	MMGBSA
S1	-6.25/30	-6.70/200	-33.17
S2	-5.88/30	-6.26/178	-46.29
S3	-6.18/11	-6.61/200	-67.28

Fig. 6. Major possible binding sites of lycorine on SINV and DENV-2 RdRp during Blind Docking (BD).

was added concurrently with the virus introduction to the cells (0 h in our study).

To understand this early effect of lycorine on we proceeded to examine the dynamics of viral RNA replication in cells infected with CHIKV and DENV, in the presence of lycorine. For DENV, we chose DENV-2 as it is the most prominent infecting serotype in India [36]. Our results show significant increase in viral RNA for both CHIKV and DENV-2 in DMSO treated cells as compared to lycorine treated cells at all time points suggesting inhibition of viral RNA synthesis by lycorine. We also noted that the quantity of viral genome at 2 hpi for CHIKV and 6 hpi for DENV-2 showed similarity between cells treated with DMSO and those treated with lycorine. This finding further validates that lycorine does not hinder viral entry. Additionally, we analysed the fold change in viral genome expression at various time points relative to the expression

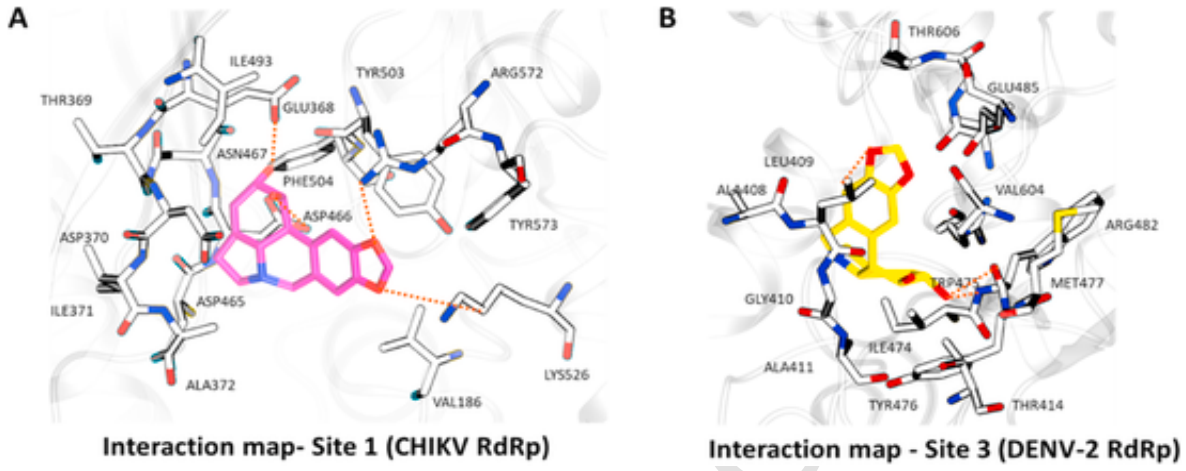

Fig. 7. Interactions between the ligand (lycorine) with SINV and DENV-2 RdRp.

in DMSO-treated cells at 2 hpi for CHIKV and 6 hpi for DENV-2 infected cells, respectively, considering it as a baseline of 1. By 8 hpi for CHIKV and 48 hpi for DENV-2, we observed an approximate 2 log10 fold increase in viral RNA in cells treated with lycorine. However, this increase was significantly lower compared to the fold increase observed in DMSO-treated cells (4.5 log10 for CHIKV and 5 log10 for DENV-2), indicating that lycorine either does not completely inhibit viral replication or the possible presence of mutant viruses that evade its inhibitory effects.

Several mechanisms have been suggested to explain how lycorine exerts its antiviral effects against different viruses. These mechanisms include hindering viral translation [22,37] inhibiting viral protease activity [38], disrupting RNA-dependent RNA polymerase (RdRp) activity [18,39], or impeding the elongation of viral polyprotein [26]. Since negative strand RNA intermediates are required as templates for positive strand RNA genome synthesis, any factor inhibiting the formation of negative strand will consequently inhibit viral replication. Thus, we analysed the expression of negative strand RNA in the presence of lycorine. We observed a significant reduction in negative strand RNA synthesis in lycorine -treated cells for both CHIKV and DENV-2. These again confirmed our time of addition results wherein adding lycorine at 0 h completely inhibited the virus. These findings also indicate a potential impairment in either the assembly of the replication complex due to the inhibition of other viral non-structural proteins or the inhibition of RdRp catalytic function by lycorine. Since the mode of action of lycorine on Zika, another flavivirus, has been shown to be the inhibition of RdRp, we proceeded to conduct molecular docking experiments on SINV and DENV-2 RdRp to identify if it is indeed the potential target for lycorine. Our docking and binding results show that lycorine binds effectively to both SINV and DENV-2 RdRp with the S1 binding site in SINV encompassing the residues in the palm domain which are crucial for RdRp catalytic activity. For DENV-2, the binding site S3 for lycorine lies in the finger domain. Both these results suggest that lycorine binds to or near to RdRp catalytic site and may inhibit the formation of both negative and positive strand RNA genome though not having binding site in same domain. Indeed, various docked poses of lycorine indicates the possibility of domain overlap sites as well, therefore, more thorough studies are needed. In a study on SARS-CoV-2 [34], it was observed that lycorine did not exhibit concentration-dependent binding with RdRp in the absence of RNA. However, once RNA was present, lycorine demonstrated a notably robust interaction. The authors further suggested that despite lycorine's small size, which initially appeared inadequate to occupy the substantially large RdRp cavity, its binding capability increased significantly in the presence of RNA due to the RNA-induced compaction of RdRp cavity, rendering it more conducive to the binding of a smaller molecule like lycorine leading to inhibition of RNA synthesis. This might explain that despite not binding to the catalytic site in DENV RdRp, lycorine might exert its effect when the positive genomic RNA strand initially binds to RdRp for generation of a negative strand template. Although our results point to inhibition of RdRp catalytic activity as the possible mode of action, our study had the limitation of not being able to perform any polymerase assay affirming a direct binding of lycorine to CHIKV and DENV RdRp and consequent inhibition of their catalytic activity.

5. Conclusion

In summary, our research illustrates that lycorine effectively inhibits both CHIKV and DENV at low micromolar concentrations by inhibiting viral RNA synthesis and this might be due to its binding to RdRp and inhibiting its catalytic function. This discovery positions lycorine as a promising broad-spectrum direct acting antiviral candidate for arboviral infections and can be used as a scaffold to develop even more potent antiviral candidate. Additional investigations such as preclinical effectiveness in animal model and toxicity studies are however necessary to validate lycorine as a safe and efficacious antiviral medication for human use in future.

Funding statement

The study was supported by Intramural funding from THSTI core grant, Translational Research Program (TRP) funded by Department of Biotechnology, India.

Data availability statement

The authors confirm that the data supporting the findings of this study are available within the article and within its supplementary material. Raw data that supports the finding of this study are available from the corresponding author upon reasonable request.

CRediT authorship contribution statement

Tanvi Agrawal: Writing – review & editing, Writing – original draft, Validation, Supervision, Methodology, Investigation, Data curation, Conceptualization. **Gazala Siddqui:** Methodology, Investigation, Formal analysis, Data curation. **Ridhima Dahiya:** Software, Methodology, Formal analysis, Data curation. **Aanchal Patidar:** Methodol-

ogy, Investigation, Formal analysis, Data curation. **Upasna Madan:** Resources. **Supratik Das:** Writing – review & editing, Resources. **Shailendra Asthana:** Writing – review & editing, Writing – original draft, Validation, Software, Methodology, Investigation, Formal analysis, Data curation. **Sweety Samal:** Writing – review & editing, Resources. **Amit Awasthi:** Writing – review & editing, Supervision, Resources, Project administration, Funding acquisition, Conceptualization.

Declaration of competing interest

None.

Acknowledgments

The following reagents was obtained through BEI Resources, NIAID, NIH: dengue Virus Type 1, 12150, NR-3785, dengue Virus Type 2, DEN2-S2, NR-15247, dengue Virus Type 4, 703-4, NR-48801. We also acknowledge the support provided by Dr Pallavi Kshetrapal, THSTI, for fluorescent microscopy.

Appendix A. Supplementary data

Supplementary data to this article can be found online at https://doi.org/10.1016/j.bbrc.2024.150393.

References

[1] S. Bhatt, P.W. Gething, O.J. Brady, J.P. Messina, A.W. Farlow, C.L. Moyes, J.M. Drake, J.S. Brownstein, A.G. Hoen, O. Sankoh, M.F. Myers, D.B. George, T. Jaenisch, G.R. Wint, C.P. Simmons, T.W. Scott, J.J. Farrar, S.I. Hay, The global distribution and burden of dengue, Nature 25 (2013) 504–517, https://doi.org/10.1038/nature12060.

[2] C. Guo, Z. Zhou, Z. Wen, Y. Liu, C. Zeng, D. Xiao, M. Ou, Y. Han, S. Huang, D. Liu, X. Ye, X. Zou, J. Wu, H. Wang, E.Y. Zeng, C. Jing, G. Yang, Global epidemiology of dengue outbreaks in 1990-2015: a systematic review and meta-analysis, Front. Cell. Infect. Microbiol. 12 (2017) 317, https://doi.org/10.3389/fcimb.2017.00317.

[3] World Health Organization, Global Strategy for Dengue Prevention and Control 2012-2020, World Health Organization, Geneva, 2012 978 92 4 150403 4.

[4] C. Schilte, F. Staikowsky, T. Couderc, Y. Madec, F. Carpentier, S. Kassab, M.L. Albert, M. Lecuit, A. Michault, Chikungunya virus-associated long-term arthralgia: a 36-month prospective longitudinal study, PLoS Neglected Trop. Dis. 7 (2013) e2137, https://doi.org/10.1371/journal.pntd.0002137.

[5] V.K. Ganesan, B. Duan, S.P. Reid, Chikungunya virus: pathophysiology, mechanism, and modeling, Viruses 9 (2017) 368, https://doi.org/10.3390/v9120368.

[6] M. Oviedo-Pastrana, N. Méndez, S. Mattar, G. Arrieta, L. Gomezcaceres, Epidemic outbreak of Chikungunya in two neighboring towns in the Colombian Caribbean: a survival analysis, Arch. Publ. Health 6 (2017) 1, https://doi.org/10.1186/s13690-016-0169-1.

[7] D.O. Andersen, N.D. Weber, S.G. Wood, B.G. Hughes, B.K. Murray, J.A. North, In vitro virucidal activity of selected anthraquinones and anthraquinone derivatives, Antivir. Res. 16 (1991) 185–196, https://doi.org/10.1016/0166-3542(91)90024-l.

[8] Y. Wang, G. Zhu, X. Li, Z. Hao, Simultaneous determination of galanthamine and lycorine in Lycoris radiata by a capillary electrophoresis with an electrochemiluminescence method, J. Separ. Sci. 37 (2014) 3007–3012, https://doi.org/10.1002/jssc.201400639.

[9] D. Lamoral-Theys, A. Andolfi, G. Van Goietsenoven, A. Cimmino, B. Le Calvé, N. Wauthoz, V. Mégalizzi, T. Gras, C. Bruyère, J. Dubois, V. Mathieu, A. Kornienko, R. Kiss, A. Evidente, Lycorine, the main phenanthridine Amaryllidaceae alkaloid, exhibits significant antitumor activity in cancer cells that display resistance to proapoptotic stimuli: an investigation of structure-activity relationship and mechanistic insight, J. Med. Chem. 22 (2009) 6244–6256, https://doi.org/10.1021/jm901031h.

[10] R.B. Giordani, B. Vieira Pde, M. Weizenmann, D.B. Rosemberg, A.P. Souza, C. Bonorino, G.A. De Carli, M.R. Bogo, J.A. Zuanazzi, T. Tasca, Lycorine induces cell death in the amitochondriate parasite, Trichomonas vaginalis, via an alternative non-apoptotic death pathway, Phytochemistry 72 (2011) 645–650, https://doi.org/10.1016/j.phytochem.2011.01.023.

[11] X. Ge, X. Meng, D. Fei, K. Kang, Q. Wang, M. Zhao, Lycorine attenuates lipopolysaccharide-induced acute lung injury through the HMGB1/TLRs/NF-κB pathway, 3 Biotech 10 (2020) 369, https://doi.org/10.1007/s13205-020-02364-5.

[12] A. Di Sotto, M. Valipour, A. Azari, S. Di Giacomo, H. Irannejad, Benzoindolizidine alkaloids tylophorine and lycorine and their analogues with antiviral, anti-Inflammatory, and anticancer properties: promises and challenges, Biomedicines 11 (2023) 2619, https://doi.org/10.3390/biomedicines11102619.

[13] Y.C. Hwang, J.J. Chu, P.L. Yang, W. Chen, M.V. Yates, Rapid identification of inhibitors that interfere with poliovirus replication using a cell-based assay, Antivir. Res. 77 (2008) 232–236, https://doi.org/10.1016/j.antiviral.2007.12.009.

[14] L. Shen, J. Niu, C. Wang, B. Huang, W. Wang, N. Zhu, Y. Deng, H. Wang, F. Ye, S. Cen, W. Tan, High-throughput screening and identification of potent broad-spectrum inhibitors of coronaviruses, J. Virol. 29 (2019), e00023 https://doi.org/10.1128/JVI.00023-19, 19.

[15] Y.N. Zhang, Q.Y. Zhang, X.D. Li, J. Xiong, S.Q. Xiao, Z. Wang, Z.R. Zhang, C.L. Deng, X.L. Yang, H.P. Wei, Z.M. Yuan, H.Q. Ye, B. Zhang, Gemcitabine, lycorine and oxysophoridine inhibit novel coronavirus (SARS-CoV-2) in cell culture, Emerg. Microb. Infect. 9 (2020) 1170–1173, https://doi.org/10.1080/22221751.2020.1772676.

[16] J. Liu, Y. Yang, Y. Xu, C. Ma, C. Qin, L. Zhang, Lycorine reduces mortality of human enterovirus 71-infected mice by inhibiting virus replication, Virol. J. 27 (2011) 483, https://doi.org/10.1186/1743-422X-8-483.

[17] D. Chen, J. Cai, J. Cheng, C. Jing, J. Yin, J. Jiang, Z. Peng, X. Hao, Design, synthesis and structure-activity relationship optimization of lycorine derivatives for HCV inhibition, Sci. Rep. 5 (2015) 14972, https://doi.org/10.1038/srep14972.

[18] H. Chen, Z. Lao, J. Xu, Z. Li, H. Long, D. Li, L. Lin, X. Liu, L. Yu, W. Liu, G. Li, J. Wu, Antiviral activity of lycorine against Zika virus in vivo and in vitro, Virology 546 (2020) 88–97, https://doi.org/10.1016/j.virol.2020.04.009.

[19] P. Wang, L.F. Li, Q.Y. Wang, L.Q. Shang, P.Y. Shi, Z. Yin, Anti-dengue-virus activity and structure-activity relationship studies of lycorine derivatives, ChemMedChem 9 (2014) 1522–1533, https://doi.org/10.1002/cmdc.201300505.

[20] G. Zou, F. Puig-Basagoiti, B. Zhang, M. Qing, L. Chen, K.W. Pankiewicz, K. Felczak, Z. Yuan, P.Y. Shi, A single-amino acid substitution in West Nile virus 2K peptide between NS4A and NS4B confers resistance to lycorine, a flavivirus inhibitor, Virology 384 (2009) 242–252, https://doi.org/10.1016/j.virol.2008.11.003.

[21] J. He, W.B. Qi, L. Wang, J. Tian, P.R. Jiao, G.Q. Liu, W.C. Ye, M. Liao, Amaryllidaceae alkaloids inhibit nuclear-to-cytoplasmic export of ribonucleoprotein (RNP) complex of highly pathogenic avian influenza virus H5N1, Influenza Other Respir Viruses 7 (2013) 922–931, https://doi.org/10.1111/irv.12035.

[22] N. Li, Z. Wang, R. Wang, Z.R. Zhang, Y.N. Zhang, C.L. Deng, B. Zhang, L.Q. Shang, H.Q. Ye, In vitro inhibition of alphaviruses by lycorine, Virol. Sin. 36 (2021) 1465–1474, https://doi.org/10.1007/s12250-021-00438-z.

[23] G. Siddqui, P. Vishwakarma, S. Saxena, V. Kumar, S. Bajpai, A. Kumar, S. Kumar, R. Khatri, J. Kaur, S. Bhattacharya, S. Ahmed, G.H. Syed, Y. Kumar, S. Samal, Aged AG129 mice support the generation of highly virulent novel mouse-adapted DENV (1-4) viruses exhibiting neuropathogenesis and high lethality, Virus Res. 341 (2024) 199331, https://doi.org/10.1016/j.virusres.2024.199331.

[24] A. Ahmadi, P. Hassandarvish, R. Lani, P. Yadollahi, A. Jokar, S.A. Bakar, K. Zandi, Inhibition of chikungunya virus replication by hesperetin and naringenin, RSC Adv. 6 (2016) 69421–69430, https://doi.org/10.1039/C6RA16640G.

[25] V.C. Maddipati, L. Mittal, M. Mantipally, S. Asthana, S. Bhattacharyya, R. Gundla, A review on the progress and prospects of dengue drug discovery targeting NS5 RNA- dependent RNA polymerase, Curr. Pharmaceut. Des. 26 (2020) 4386–4409, https://doi.org/10.2174/1381612826666200523174753.

[26] T.L. Yap, T. Xu, Y.L. Chen, H. Malet, M.P. Egloff, B. Canard, S.G. Vasudevan, J. Lescar, Crystal structure of the dengue virus RNA-dependent RNA polymerase catalytic domain at 1.85-angstrom resolution, J. Virol. 81 (2007) 4753–4765, https://doi.org/10.1128/JVI.02283-06.

[27] M.C.L.C. Freire, L.G.M. Basso, L.F.S. Mendes, N.C.M.R. Mesquita, M. Mottin, R.S. Fernandes, L.R. Policastro, A.S. Godoy, I.A. Santos, U.E.A. Ruiz, I.P. Caruso, B.K.P. Sousa, A.C.G. Jardim, F.C.L. Almeida, L.H.V.G. Gil, C.H. Andrade, G. Oliva, Characterization of the RNA-dependent RNA polymerase from Chikungunya virus and discovery of a novel ligand as a potential drug candidate, Sci. Rep. 12 (2022) 10601, https://doi.org/10.1038/s41598-022-14790-x.

[28] W.L. Jorgensen, D.S. Maxwell, J. Tirado-Rives, Development and testing of the OPLS all-atom force field on conformational energetics and properties of organic liquids, J. Am. Chem. Soc. 118 (1996) 11225–11236, https://doi.org/10.1021/ja9621760.

[29] G.M. Morris, R. Huey, W. Lindstrom, M.F. Sanner, R.K. Belew, D.S. Goodsell, A.J. Olson, AutoDock4 and AutoDockTools4: automated docking with selective receptor flexibility, J. Comput. Chem. 30 (2009) 2785–2791, https://doi.org/10.1002/jcc.21256.

[30] V.C. Maddipati, L. Mittal, J. Kaur, Y. Rawat, C.P. Koraboina, S. Bhattacharyya, S. Asthana, R. Gundla, Discovery of non-nucleoside oxindole derivatives as potent inhibitors against dengue RNA-dependent RNA polymerase, Bioorg. Chem. 131 (2023) 106277, https://doi.org/10.1016/j.bioorg.2022.106277.

[31] L. Mittal, A. Kumari, C. Suri, S. Bhattacharya, S. Asthana, Insights into structural dynamics of allosteric binding sites in HCV RNA-dependent RNA polymerase, J. Biomol. Struct. Dyn. 38 (2020) 1612–1625, https://doi.org/10.1080/07391102.2019.1614480.

[32] E.V.S. Reis, B.M. Damas, D.C. Mendonça, J.S. Abrahão, C.A. Bonjardim, In-depth characterization of the chikungunya virus replication cycle, J. Virol. 96 (2022) e0173221, https://doi.org/10.1128/JVI.01732-21.

[33] T.J. Chambers, C.S. Hahn, R. Galler, C.M. Rice, Flavivirus genome organization, expression, and replication, Annu. Rev. Microbiol. 44 (1990) 649–688, https://doi.org/10.1146/annurev.mi.44.100190.003245.

[34] Z. Yao, S. Ramachandran, S. Huang, Y. Jami-Alahmadi, J.A. Wohlschlegel, M.M.H. Li, Chikungunya virus glycoproteins transform macrophages into productive viral dissemination vessels, bioRxiv [Preprint] 29 (2023) 2023 https://doi.org/10.1101/2023.05.29.542714, 05.29.542714.

[35] K. Labadie, T. Larcher, C. Joubert, A. Mannioui, B. Delache, P. Brochard, L.

Guigand, L. Dubreil, P. Lebon, B. Verrier, X. de Lamballerie, A. Suhrbier, Y. Cherel, R. Le Grand, P. Roques, Chikungunya disease in nonhuman primates involves long-term viral persistence in macrophages, J. Clin. Invest. 120 (2010) 894–906, https://doi.org/10.1172/JCI40104.

[36] A. Anantharaj, T. Agrawal, P.K. Shashi, A. Tripathi, P. Kumar, I. Khan, M. Pareek, B. Singh, C. Pattabiraman, S. Kumar, R. Pandey, A. Chandele, R. Lodha, S.S. Whitehead, G.R. Medigeshi, Neutralizing antibodies from prior exposure to dengue virus negatively correlate with viremia on re-infection, Commun. Med. 9 (2023) 148, https://doi.org/10.1038/s43856-023-00378-7.

[37] P.X. Ren, W.J. Shang, W.C. Yin, H. Ge, L. Wang, X.L. Zhang, B.Q. Li, H.L. Li, Y.C. Xu, E.H. Xu, H.L. Jiang, L.L. Zhu, L.K. Zhang, F. Bai, A multi-targeting drug design strategy for identifying potent anti-SARS-CoV-2 inhibitors, Acta Pharmacol. Sin. 43 (2022) 483–493, https://doi.org/10.1038/s41401-021-00668-7.

[38] B. Kurt, Investigation of the potential inhibitor effects of lycorine on Sars-Cov-2 main protease (Mpro) using molecular dynamics simulations and MMPBSA, Inter J Life Sci Biotech 5 (2022) 424–435, https://doi.org/10.38001/ijlsb.1110761.

[39] Y.H. Jin, J.S. Min, S. Jeon, J. Lee, S. Kim, T. Park, D. Park, M.S. Jang, C.M. Park, J.H. Song, H.R. Kim, S. Kwon, Lycorine, a non-nucleoside RNA dependent RNA polymerase inhibitor, as potential treatment for emerging coronavirus infections, Phytomedicine 86 (2021) 153440, https://doi.org/10.1016/j.phymed.2020.153440.